



# LUND UNIVERSITY

## On the numerical evaluation of stress intensity factors for an interface crack of a general shape

Helsing, Johan

*Published in:*  
International Journal for Numerical Methods in Engineering

*DOI:*  
[10.1002/\(SICI\)1097-0207\(19990220\)44:5<729::AID-NME529>3.0.CO;2-A](https://doi.org/10.1002/(SICI)1097-0207(19990220)44:5<729::AID-NME529>3.0.CO;2-A)

1999

[Link to publication](#)

*Citation for published version (APA):*  
Helsing, J. (1999). On the numerical evaluation of stress intensity factors for an interface crack of a general shape. *International Journal for Numerical Methods in Engineering*, 44(5), 729-741.  
[https://doi.org/10.1002/\(SICI\)1097-0207\(19990220\)44:5<729::AID-NME529>3.0.CO;2-A](https://doi.org/10.1002/(SICI)1097-0207(19990220)44:5<729::AID-NME529>3.0.CO;2-A)

*Total number of authors:*  
1

### General rights

Unless other specific re-use rights are stated the following general rights apply:  
Copyright and moral rights for the publications made accessible in the public portal are retained by the authors and/or other copyright owners and it is a condition of accessing publications that users recognise and abide by the legal requirements associated with these rights.

- Users may download and print one copy of any publication from the public portal for the purpose of private study or research.
- You may not further distribute the material or use it for any profit-making activity or commercial gain
- You may freely distribute the URL identifying the publication in the public portal

Read more about Creative commons licenses: <https://creativecommons.org/licenses/>

### Take down policy

If you believe that this document breaches copyright please contact us providing details, and we will remove access to the work immediately and investigate your claim.

LUND UNIVERSITY

PO Box 117  
221 00 Lund  
+46 46-222 00 00

# On the numerical evaluation of stress intensity factors for an interface crack of a general shape

Johan Helsing

Department of Solid Mechanics, Royal Institute of Technology,  
SE-100 44 Stockholm, Sweden

and

Department of Scientific Computing

Uppsala University  
SE-751 04 Uppsala, Sweden

February 20, 1998, revised June 17, 1998

## Abstract

A numerical algorithm is presented for the problem of a crack along the interface of an elastic inclusion embedded in an elastic plane subjected to uniform stress at infinity. The algorithm is based on a Fredholm integral equation of the second kind and allows for fast and accurate solutions to geometries of great complexity. In an example crack opening displacement and stress intensity factors are computed for a crack in the interface of an inclusion with nineteen protruding arms.

## 1 Introduction

Over the years much work has been devoted to the evaluation of stress intensity factors for composite materials with interface cracks. For two simple configurations – one interface crack between either a circular elastic inclusion or an elliptical rigid inclusion, and an elastic plane – closed form solutions are available [1, 2, 3]. Numerical algorithms are needed for interface cracks with more complicated shapes.

The problem of constructing an efficient general algorithm for the numerical computation of stress intensity factors in cracked composites is indeed a formidable one. The leading numerical algorithm, until now, may very well be the so called “body force method” used recently by Chen and Nakamichi [4]. The authors solve the problem of a crack in the interface of an elastic ellipse in an elastic plane. The implementation is based on a fundamental solution for a point-force outside an ellipse. The relative error in the computations is of the order of one per cent.

In this paper we present a Fredholm integral equation for the interface crack problem. We solve the integral equation numerically with a Nyström algorithm. Our work improves on that of the state of the art in the field in several ways:

- by using an abstract layer potential (avoiding geometry-specific fundamental solutions) we are able to treat an elastic inclusion of a general shape

- by solving for an unknown density that is related to the crack opening displacement (not to its derivative) we can retrieve the crack opening displacement with great ease
- by using an integral equation of Fredholm's second kind (not of Fredholm's first kind) we get a numerically stable algorithm. Roughly speaking, this means that we can get the same accuracy for quantities related to the solution, such as stress intensity factors, as we get for quantities related to the geometry itself, such as the arclength of the crack.

The paper is organized as follows: Section 2 presents our original choice of complex representation for the stress field in the material along with a first kind Fredholm integral equation for an unknown layer potential. This integral equation is transformed into a second kind integral equation in Section 3. An alternative representation is introduced in Section 4 leading to a slightly simpler integral equation. Section 5 discusses the numerical evaluation of singular integral operators and Section 6 concerns the calculation of quadrature weights. In section 7 certain weights are factorized out from the layer potential so that the solution to the integral equation becomes a smooth function. Section 8 explains how to extract stress intensity factors and crack opening displacement from this solution. Section 9 contains numerical results along with timings. For simple shapes of interfaces and cracks we get convergence to about twelve digits in IEEE double precision arithmetic. A typical calculation takes around three seconds on a SUN Ultra 1 workstation.

## 2 Complex potentials and integral operators

Let  $U$  denote the Airy stress function for a locally isotropic two-dimensional linearly elastic material with an inclusion and an interface crack. External forces are applied at infinity. Since  $U$  satisfies the biharmonic equation everywhere (outside the inclusion interface) it can be represented as

$$U = \Re\{\bar{z}\phi + \chi\}, \quad (1)$$

where  $\phi$  and  $\chi$  are analytic functions of the complex variable  $z$  and  $\Re\{f\}$  denotes the real part of the function  $f$ . For a thorough discussion of the complex variable approach to crack problems in elasticity, see Muskhelishvili [5], Mikhlin [6], and Milne-Thompson [7]. For our purposes it is sufficient to observe a few relations that link the complex potentials to quantities of physical interest: The displacement  $(u_x, u_y)$  in the material satisfies

$$u_x + iu_y = \left(\frac{1}{2\mu} + \frac{1}{\kappa}\right)\phi - \frac{1}{2\mu}(z\bar{\phi}' + \bar{\psi}), \quad (2)$$

where  $\psi = \chi'$ ,  $\kappa$  is the two-dimensional bulk modulus, and  $\mu$  is the two-dimensional shear modulus. The integral of the traction  $(t_x, t_y)$  along a curve  $\Gamma(s)$  with normal  $(n_x, n_y)$  can be obtained from the relation

$$\int_{\Gamma(s_0)}^{\Gamma(s)} (t_x + it_y) ds = - \Big|_{s_0}^s i \left( \phi + z\bar{\phi}' + \bar{\psi} \right), \quad (3)$$

where  $s$  denotes arclength. Complex differentiation of the expression (2) along the tangent to  $\Gamma(s)$  gives

$$\frac{d}{dz}(u_x + iu_y) = \left(\frac{1}{2\mu} + \frac{1}{\kappa}\right)\Phi - \frac{1}{2\mu}\left(\bar{\Phi} - \frac{\bar{n}}{n}z\bar{\Phi}' - \frac{\bar{n}}{n}\bar{\Psi}\right), \quad (4)$$

where  $n = n_x + in_y$ ,  $\Phi = \phi'$ , and  $\Psi = \chi''$ . Differentiation with respect to arclength in (3) gives

$$t_x + it_y = \Phi n + \overline{\Phi} \bar{n} - z \overline{\Phi'} \bar{n} - \overline{\Psi} \bar{n}, \quad (5)$$

Consider now an infinite medium with elastic moduli  $\kappa_1$  and  $\mu_1$  which surrounds an inclusion with elastic moduli  $\kappa_2$  and  $\mu_2$ . The interface of the inclusion,  $\Gamma$ , consists of a cracked segment  $\Gamma_{\text{cr}}$  and a bonded segment  $\Gamma_{\text{bo}}$ . We refer to  $\Gamma_{\text{cr}}$  and  $\Gamma_{\text{bo}}$  as *crack* and *bond*. The starting point of the crack,  $\gamma_s$ , and the endpoint of the crack,  $\gamma_e$ , are called crack tips. The stress at infinity is  $\sigma^\infty = (\sigma_{xx}, \sigma_{yy}, \sigma_{xy})$ . We would like compute the displacement and stress fields in the material subject to three different imposed stresses at infinity, namely  $\sigma_{xx}^\infty = (1, 0, 0)$ ,  $\sigma_{yy}^\infty = (0, 1, 0)$ , and  $\sigma_{xy}^\infty = (0, 0, 1)$ . Since the equations of elasticity are satisfied everywhere except for at  $\Gamma$ , and assuming the crack opening displacement is non-negative, it remains to solve a problem which consists of enforcing zero traction along the crack and continuity of traction and displacement along the bond.

A standard starting point for crack and inclusion problems is to work with (4) and (5) and to represent the upper-case potentials  $\Phi$  and  $\Psi$  as Cauchy-type integrals:

$$\Phi(z) = \frac{1}{2\pi i} \int_{\Gamma} \frac{\Omega(\tau)w(\tau)d\tau}{\tau - z} + \frac{\alpha}{2}, \quad (6)$$

and

$$\Psi(z) = -\frac{1}{2\pi i} \int_{\Gamma} \frac{\overline{\Omega(\tau)w(\tau)d\bar{\tau}}}{\tau - z} - \frac{1}{2\pi i} \int_{\Gamma} \frac{\bar{\tau}\Omega(\tau)w(\tau)d\tau}{(\tau - z)^2} + \beta, \quad (7)$$

where  $\Omega$  is an unknown density on  $\Gamma$  and  $w$  is a weight function, introduced for convenience, and given in (16) below.

**Remark 2.1** The constants  $\alpha$  and  $\beta$  in (6) and (7) represent the forcing terms in our formulation. For imposed stresses  $\sigma_{xx}^\infty$ ,  $\sigma_{yy}^\infty$ , and  $\sigma_{xy}^\infty$  the constants take the values  $\alpha = 1/2$  and  $\beta = -1/2$ ,  $\alpha = 1/2$  and  $\beta = 1/2$ , and  $\alpha = 0$  and  $\beta = i$ . In the following, the constant  $\alpha$  is assumed to be real valued.

Once  $\Phi$  is assumed to take the form (6), the expression (7) for  $\Psi$  enforces continuity of traction across the interface. The requirements of continuity of displacement along the bond, zero traction along the crack, closure of the crack and Lemma 2.1 below, lead to an integral equation for  $\Omega(z)$ :

$$(K + CM_3)\Omega(z) = -B\alpha - C\frac{\bar{n}}{n}\bar{\beta}, \quad z \in \Gamma, \quad (8)$$

$$Q\Omega = 0. \quad (9)$$

Here  $K$  and  $M_3$  are integral operators given by

$$K\Omega(z) = A(z)w(z)\Omega(z) + \frac{B(z)}{\pi i} \int_{\Gamma} \frac{\Omega(\tau)w(\tau)d\tau}{\tau - z}, \quad (10)$$

and

$$M_3\Omega(z) = \frac{1}{2\pi i} \left[ \int_{\Gamma} \frac{\Omega(\tau)w(\tau)d\tau}{\tau - z} \right]$$

$$\left. + \frac{\bar{n}}{n} \int_{\Gamma} \frac{\Omega(\tau)w(\tau)d\tau}{\bar{\tau} - \bar{z}} + \int_{\Gamma} \frac{\overline{\Omega(\tau)w(\tau)}d\bar{\tau}}{\bar{\tau} - \bar{z}} + \frac{\bar{n}}{n} \int_{\Gamma} \frac{(\tau - z)\overline{\Omega(\tau)w(\tau)}d\bar{\tau}}{(\bar{\tau} - \bar{z})^2} \right]. \quad (11)$$

Despite appearances, the operator  $M_3$  has a continuous integrand, while the operator  $K$  is to be interpreted in the Cauchy principal value sense. The functions  $A(z)$ ,  $B(z)$ , and  $C(z)$  are piece-wise constant and given by

$$\begin{aligned} A(z) &= 1, & z \in \Gamma_{\text{bo}}, & \quad \text{and} & \quad A(z) = 0, & \quad z \in \Gamma_{\text{cr}}, \\ B(z) &= d_1, & z \in \Gamma_{\text{bo}}, & \quad \text{and} & \quad B(z) = 1, & \quad z \in \Gamma_{\text{cr}}, \\ C(z) &= d_2, & z \in \Gamma_{\text{bo}}, & \quad \text{and} & \quad C(z) = -1, & \quad z \in \Gamma_{\text{cr}}. \end{aligned} \quad (12)$$

The constants  $d_1$  and  $d_2$  are given by

$$d_1 = \left( \frac{1}{\kappa_2} - \frac{1}{\kappa_1} \right) / \left( \frac{1}{\mu_2} + \frac{1}{\kappa_2} + \frac{1}{\mu_1} + \frac{1}{\kappa_1} \right),$$

and

$$d_2 = \left( \frac{1}{\mu_2} - \frac{1}{\mu_1} \right) / \left( \frac{1}{\mu_2} + \frac{1}{\kappa_2} + \frac{1}{\mu_1} + \frac{1}{\kappa_1} \right). \quad (13)$$

The operator  $Q$  is a mapping from  $\Gamma$  into the complex numbers given by

$$Q\Omega = \frac{1}{\pi i} \int_{\Gamma} \Omega(z)w(z)dz. \quad (14)$$

**Lemma 2.1** *For any function  $f(z)$*

$$\frac{1}{\pi i} \int_{\Gamma} M_3 f(z)dz = -Qf \quad (15)$$

*Proof:* The lemma is proved by changing the order of integration in the double intergral.  $\square$

A convenient choice for the weight function  $w(z)$  can now be made. On  $\Gamma$  it is given by

$$w(z) = (A(z) - B(z))(z - \gamma_s)^{\bar{a}}(z - \gamma_e)^a, \quad z \in \Gamma, \quad (16)$$

where the complex exponent  $a$  is

$$a = -\frac{1}{2} + \frac{i}{2\pi} \log \left( \frac{1 - d_1}{1 + d_1} \right) \quad (17)$$

The weight function  $w(z)$  is the limit from the right (relative to the orientation of  $\Gamma$ ) of the branch given by a branch cut along  $\Gamma$  and

$$\lim_{z \rightarrow \infty} z(z - \gamma_s)^{\bar{a}}(z - \gamma_e)^a = 1. \quad (18)$$

A less common option for crack problems, but one that has shown to be numerically more efficient in the presence of inclusions [8, 9], is to work with (2) and (3) and to represent the lower-case potentials  $\phi$  and  $\psi$  in the form

$$\phi(z) = \frac{1}{2\pi i} \int_{\Gamma} \frac{\omega(\tau)v(\tau)d\tau}{\tau - z} + \frac{\alpha z}{2} + \frac{c_0}{2}, \quad (19)$$

and

$$\psi(z) = \frac{1}{2\pi i} \int_{\Gamma} \frac{\omega(\tau)v(\tau)d\bar{\tau}}{\tau - z} - \frac{1}{2\pi i} \int_{\Gamma} \frac{\overline{\omega(\tau)v(\tau)}d\tau}{\tau - z} - \frac{1}{2\pi i} \int_{\Gamma} \frac{\bar{\tau}\omega(\tau)v(\tau)d\tau}{(\tau - z)^2} + \beta z + \frac{\bar{c}_0}{2}, \quad (20)$$

where  $c_0$  is a complex constant corresponding to rigid body displacement and where  $\omega$  is an unknown density related to the density  $\Omega$  through the relation

$$\Omega(z)w(z) = \frac{d}{dz} (\omega(z)v(z)), \quad (21)$$

and  $v$  is a weight function given in (31) below. We will return to this option in Section 4.

### 3 A Fredholm equation

We now intend to rewrite the system (8) and (9) as one Fredholm integral equation of the second kind. For this we need a few new functions and operators. Let

$$A^*(z) = \frac{A(z)}{A^2(z) - B^2(z)}, \quad \text{and} \quad B^*(z) = \frac{B(z)}{A^2(z) - B^2(z)}. \quad (22)$$

Let  $K^*$  be an operator whose action on a function  $f(z)$  is defined by

$$K^*f(z) = \frac{A^*(z)f(z)}{w(z)} - \frac{B^*(z)}{\pi i} \int_{\Gamma} \frac{f(\tau)d\tau}{w(\tau)(\tau - z)}. \quad (23)$$

Let  $P_{\text{cr}}$  and  $P_{\text{bo}}$  be two projection operators which project onto the crack and the bond, respectively.

The following lemma is proved with relations in Paragraphs 107 and 117 of Ref. [10] and with techniques used in Appendix I of Ref. [2] and in Section 4 of Ref. [9].

#### Lemma 3.1

$$K^*P_{\text{cr}}B = B^*(1 + d_1)(z + \bar{a}\gamma_s + a\gamma_e) - w^{-1}d_1, \quad (24)$$

$$K^*P_{\text{bo}}B = -B^*d_1(z + \bar{a}\gamma_s + a\gamma_e) + w^{-1}d_1, \quad (25)$$

$$QB^* = 1, \quad (26)$$

$$Q \circ K^* = 0, \quad (27)$$

$$K \circ K^* = I, \quad (28)$$

$$K^* \circ K = I - B^* \circ Q. \quad (29)$$

**Theorem 1** *The system given by (8) and (9) is equivalent with the following single Fredholm integral equation of the second kind.*

$$(I + K^* \circ CM_3)\Omega(z) = -K^* \left( B\alpha + C \frac{\bar{n}}{n} \bar{\beta} \right), \quad z \in \Gamma. \quad (30)$$

*Proof:* If we apply  $K^*$  to the left in (8), use (29), and incorporate (9) we get (30). If we apply  $K$  to the left in (30) and use (28) we get back (8). If we apply  $Q$  to the left in (30) and use (27) we get back (9).  $\square$

## 4 An alternative formulation

We now return to the representation (19) and (20) for the lower-case potentials  $\phi$  and  $\psi$ . First, we need to introduce some new notation. Let  $v$  be a weight which on  $\Gamma$  is defined by

$$v(z) = (A(z) - B(z))(z - \gamma_s)\bar{b}(z - \gamma_e)^b, \quad z \in \Gamma, \quad (31)$$

where

$$b = \frac{1}{2} + \frac{i}{2\pi} \log \left( \frac{1 - d_1}{1 + d_1} \right). \quad (32)$$

Let  $L$  be an operator defined by

$$L\omega(z) = A(z)v(z)\omega(z) + \frac{B(z)}{\pi i} \int_{\Gamma} \frac{\omega(\tau)v(\tau)d\tau}{\tau - z}, \quad (33)$$

and let  $L^*$  be an operator whose action on a function  $f(z)$  is defined by

$$L^*f(z) = \frac{A^*(z)f(z)}{v(z)} - \frac{B^*(z)}{\pi i} \int_{\Gamma} \frac{f(\tau)d\tau}{v(\tau)(\tau - z)}. \quad (34)$$

A new smooth operator  $M_2$  is introduced as

$$M_2\omega(z) = \frac{1}{2\pi i} \int_{\Gamma} \omega(\tau)v(\tau)d \left[ \log \frac{\tau - z}{\bar{\tau} - \bar{z}} \right] + \frac{1}{2\pi i} \int_{\Gamma} \overline{\omega(\tau)v(\tau)}d \left[ \frac{\tau - z}{\bar{\tau} - \bar{z}} \right]. \quad (35)$$

The operator  $R$  is a mapping from  $\Gamma$  into the complex numbers given by

$$R\omega = \frac{1}{\pi i} \int_{\Gamma} \frac{\omega(z)dz}{v(z)}. \quad (36)$$

The following lemma is proved with the same methods as Lemma 3.1.

### Lemma 4.1

$$L^*P_{\text{cr}}B = -v^{-1}d_1, \quad (37)$$

$$L^*P_{\text{bo}}B = v^{-1}d_1, \quad (38)$$

$$RB = -1, \quad (39)$$

$$L^* \circ L = I, \quad (40)$$

$$L \circ L^* = I + B \circ R. \quad (41)$$

Once  $\phi$  is assumed to take the form (19), the expression (20) for  $\psi$  enforces the continuity of the integral of traction across the interface. The requirements of zero traction along the crack and of continuity of displacement along the bond lead to the integral equation for  $\omega(z)$

$$(L + CM_2)\omega(z) = -B\alpha z + C\bar{\beta}\bar{z} + c_0B, \quad z \in \Gamma, \quad (42)$$

where  $c_0$  is determined by the consistency condition

$$R \circ CM_2\omega(z) = R(-B\alpha z + C\bar{\beta}\bar{z} + c_0B). \quad (43)$$

**Theorem 2** *The system given by (42) and (43) is equivalent with the following single Fredholm integral equation of the second kind.*

$$(I + L^* \circ CM_2)\omega(z) = L^*(-B\alpha z + C\bar{\beta}\bar{z}), \quad z \in \Gamma. \quad (44)$$

*Proof:* If we apply  $L^*$  to the left in (42) and use (40) we get (44). If we apply  $L$  to the left in (44) and use (41) we get back (42) and (43).  $\square$

## 5 Evaluation of singular integral operators

Let us evaluate the operator  $K^*$  of (23) acting on a function  $f$  on the form  $f(z) = C(z)g(z)$ , where  $g$  is smooth. Using (24) and (25) one can write

$$K^*f(z) = B^*K_1^*f(z) + (d_1 + d_2)w(z)^{-1}g(z), \quad (45)$$

where

$$K_1^*f(z) = -g(z)(1 + d_1 + d_2)(z + \bar{a}\gamma_s + a\gamma_e) - \frac{1}{\pi i} \int_{\Gamma} \frac{(g(\tau) - g(z))C(\tau)d\tau}{(\tau - z)w(\tau)}. \quad (46)$$

Similarly, the operator  $L^*$  of (34) acting on a function  $f$  on the form  $f(z) = C(z)g(z)$  can be evaluated using (37) and (38) as

$$L^*f(z) = B^*L_1^*f(z) + (d_1 + d_2)v(z)^{-1}g(z), \quad (47)$$

where

$$L_1^*f(z) = -\frac{1}{\pi i} \int_{\Gamma} \frac{(g(\tau) - g(z))C(\tau)d\tau}{(\tau - z)v(\tau)}. \quad (48)$$

**Remark 5.1** The integrands in the above integrals are smooth. The weight functions are piece-wise smooth. Therefore the integrals can be evaluated numerically to high precision using composite quadrature.

## 6 Quadrature

We present a quadrature rule for a quadrature panel containing a crack tip. We chose a panel that contains the crack tip  $\gamma_s$  and consider the weight function  $w(z)$  of (16). Other cases can be treated in a similar fashion. The singularity at  $\gamma_s$  is governed by the exponent  $\bar{a}$ . Take the nodes  $x_i$ ,  $i = 1, \dots, N$ , to be the zeros in  $[-1, 1]$  of the Legendre polynomial  $P_N(x)$ . After a suitable transformation of the integrand and the integration interval we are faced with the problem of finding complex valued weights  $h_i$ ,  $i = 1, \dots, N$ , such that

$$\int_{-1}^1 f(x)(x+1)^{\bar{a}}dx \approx \sum_{i=1}^N f(x_i)h_i. \quad (49)$$

$N - 1$  order accurate weights  $h_i$  can be computed by analytic integration of the Legendre interpolating polynomial through the points  $(x_i, f(x_i))$ ,  $i = 1, \dots, N$ , and use of the formula

$$\int_{-1}^1 (x+1)^{\bar{a}}x^n dx = 2^{(\bar{a}+1)}(-1)^n \sum_{k=0}^n \frac{(-2)^k}{(k + \bar{a} + 1)} \binom{n}{k}. \quad (50)$$

A few digits will be lost in the numerical evaluation of the  $N$  weights  $h_i$  due to cancellation in (50). For best possible accuracy we recommend quadruple precision arithmetic for the calculation of the weights  $h_i$  and regular double precision arithmetic for all other numerical calculations. This strategy has been used in the present paper.

**Remark 6.1** For the case  $\Im\{\bar{a}\} = 0$  one can make the quadrature  $2N - 1$  order accurate by using the zeros of the Jacobi polynomials  $P_N^{(0,-0.5)}(x)$  as nodes, rather than the zeros of  $P_N(x)$ . It is possible that Jacobi nodes would be more efficient than Legendre nodes also when  $\Im\{\bar{a}\} \neq 0$ , but for simplicity we use Legendre nodes on all panels.

## 7 Solving for a smooth unknown function

When  $M_3$  operates on any function, the result is a smooth function. When  $K^*$  operates on a function  $C(z)g(z)$ , where  $g$  is smooth, the result is not smooth. It follows from (45) and (30) that  $\Omega$  can be represented as  $\Omega = B^*\Omega_I + (d_1 + d_2)w^{-1}\Omega_{II}$ , where  $\Omega_I$  and  $\Omega_{II}$  are smooth. For this reason we expand (30) as

$$\left( \begin{bmatrix} I & 0 \\ 0 & I \end{bmatrix} + \begin{bmatrix} K_I^* \circ CM_3 & 0 \\ 0 & M_3 \end{bmatrix} \begin{bmatrix} B^* & (d_1 + d_2)w^{-1} \\ B^* & (d_1 + d_2)w^{-1} \end{bmatrix} \right) \begin{pmatrix} \Omega_I \\ \Omega_{II} \end{pmatrix} = \begin{pmatrix} -\alpha(z + \bar{a}\gamma_s + a\gamma_e) - K_I^* C \frac{\bar{n}}{n} \bar{\beta} \\ -\frac{\bar{n}}{n} \bar{\beta} \end{pmatrix}. \quad (51)$$

Similarly, for the lower-case potentials, we represent  $\omega$  as  $\omega = B^*\omega_I + (d_1 + d_2)v^{-1}\omega_{II}$  and expand (44) as

$$\left( \begin{bmatrix} I & 0 \\ 0 & I \end{bmatrix} + \begin{bmatrix} L_I^* \circ CM_2 & 0 \\ 0 & M_2 \end{bmatrix} \begin{bmatrix} B^* & (d_1 + d_2)v^{-1} \\ B^* & (d_1 + d_2)v^{-1} \end{bmatrix} \right) \begin{pmatrix} \omega_I \\ \omega_{II} \end{pmatrix} = \begin{pmatrix} -\alpha + L_I^* C \bar{z} \bar{\beta} \\ \bar{z} \bar{\beta} \end{pmatrix} \quad (52)$$

**Remark 7.1** It is not necessary to solve (51) and (52) as they stand. For example, (52) can be rewritten as an integral equation for  $\omega_{II}$  only

$$(I + M_2 \circ L^* C)\omega_{II}(z) = \bar{z}\bar{\beta} + \alpha M_2 B^*. \quad (53)$$

Once this equation is solved  $\omega_I$  can be computed from

$$\omega_I(z) = -\alpha + L_I^* C \omega_{II}(z). \quad (54)$$

## 8 Stress intensity factors and crack opening displacement

The derivative of the opening displacement at crack  $\Gamma$  can be expressed in terms of  $\Omega(z)$  via (4). The stress intensity factor  $F_I + iF_{II}$  at the crack tips  $\gamma_s$  and  $\gamma_e$  can be defined as [11]

$$F_I + iF_{II} = -\frac{i\sqrt{2\pi}}{g_s} \sin(\pi a) \lim_{z \rightarrow \gamma_s} B^*(z) \frac{\overline{w(z)}}{s(z)^a} \lim_{z \rightarrow \gamma_s} \overline{\Omega_I(z)},$$

and

$$F_{\text{I}} + iF_{\text{II}} = \frac{i\sqrt{2\pi}}{g_e} \sin(\pi a) \lim_{z \rightarrow \gamma_e} B^*(z) \frac{\overline{w(z)}}{s(z)^{\bar{a}}} \lim_{z \rightarrow \gamma_e} \overline{\Omega_{\text{I}}(z)}, \quad (55)$$

where  $s$  is arclength measured from the closest crack-tip, and  $g_s$  and  $g_e$  are optional normalization factors which may include the average applied stress. The first limits in equations (55) can be evaluated analytically, the second limits numerically.

From (21) and (55) follow expressions for the stress intensity factors in terms of  $\omega$

$$F_{\text{I}} + iF_{\text{II}} = -\frac{b\sqrt{2\pi}}{g_s} \sin(\pi b) \lim_{z \rightarrow \gamma_s} n(z) B^*(z) \frac{\overline{v(z)}}{s(z)^{\bar{b}}} \lim_{z \rightarrow \gamma_s} \overline{\omega_{\text{I}}(z)},$$

and

$$F_{\text{I}} + iF_{\text{II}} = -\frac{\bar{b}\sqrt{2\pi}}{g_e} \sin(\pi b) \lim_{z \rightarrow \gamma_e} n(z) B^*(z) \frac{\overline{v(z)}}{s(z)^{\bar{b}}} \lim_{z \rightarrow \gamma_e} \overline{\omega_{\text{I}}(z)}. \quad (56)$$

From (2) and (42) follows an expression for the crack opening displacement

$$\delta u_x + i\delta u_y = -\frac{1}{2} \left( \frac{1}{\mu_2} + \frac{1}{\kappa_2} + \frac{1}{\mu_1} + \frac{1}{\kappa_1} \right) (\omega(z)v(z) - (d_1 + d_2)(\bar{\beta}\bar{z} - M_2\omega(z))). \quad (57)$$

## 9 Numerical results

In this section we will solve (51) and (52) for three different examples involving interface cracks. The two first examples – the elastic circle and the elastic ellipse – are simple. The purpose of solving these examples is to validate our algorithm against results in the literature. The third example – an inclusion with nineteen protruding arms – is more complex. The purpose of solving this example is to demonstrate the stability of our method and to investigate which of the two formulations (51) and (52) is the most efficient.

We will solve (51) and (52) using a Nyström algorithm with composite quadrature and the GMRES iterative solver [12]. On quadrature panels that do not contain crack tips we use 16 point Gaussian quadrature. On panels that do contain a crack tip we use the quadrature described in Section 6 with  $N = 16$ . Our procedure for determining the number of accurate digits is as follows: we start out with a given number,  $m$  say, of quadrature panels of equal length, we solve the integral equations, and we compute the stress intensity factors. Then we repeat this procedure for  $2m$  panels, for  $3m$  panels, and so on. As a result we can see the stress intensity factors converge digit by digit to values that do not change with further resolution. Beyond a certain level of resolution convergence stops and we arrive at the final accuracy presented in the examples below.

### 9.1 A circular inclusion

Let us look at an inclusion in the shape of a disk with radius  $R$  embedded in an infinite medium. The disk is placed at the origin of the complex plane. A uniaxial stress  $\sigma_{yy}^\infty$  is applied at infinity. In the interface there is a crack of length  $2l$ . The normalization factors in (55) are chosen as

$$g_s = -\frac{\bar{a}\sqrt{2\pi}}{\sigma_{yy}^\infty(2l)^{\bar{a}}}, \quad \text{and} \quad g_e = -\frac{a\sqrt{2\pi}}{\sigma_{yy}^\infty(2l)^a},$$

The problem of determining the stress intensity factors for this setup, with varying opening angles and elastic moduli, has a (rather complicated) analytical solution [13, 4]. The stress intensity factors have also been calculated numerically and tabulated for a few cases by Chen and Nakamichi [4] using a method based on a series expansions of the fundamental solution for a point-force outside an elliptical inclusion in an infinite plate. The relative error in these calculations is on the order of one per cent.

For comparison we first choose a crack that starts at  $\gamma_s = -iR$ , follows the interface counter-clockwise, and ends at  $\gamma_e = -R$  so that the length of the crack is  $3\pi R/2$ . The elastic moduli of the surrounding medium are  $\kappa_1 = 2.5$  and  $\mu_1 = 1$ . The elastic moduli of the disk are  $\kappa_2 = 5$  and  $\mu_2 = 2$ . At crack tip  $\gamma_e$  Chen and Nakamichi get  $F_I = 0.2374$  and  $F_{II} = 0.3838$ . With three, or more, quadrature panels each on the crack and on the bonded interface and four iterations in the GMRES solver we get  $F_I = 0.2400348149934$  and  $F_{II} = 0.3863270862335$ , both with the formulation of equation (51) and the formulation of equation (52). The computation time on a SUN Ultra 1 workstation was about one second. In the table of Chen and Nakamichi [4] there are 36 numerical entries corresponding to analytical solutions for different opening angles and orientations of the interface crack. We reproduced all the digits in all the entries except for the one labeled  $F_{IB}$ ,  $\theta_C^\circ = 45$ ,  $\omega^\circ = 45$  where we suspect that the authors have confused the result of their own calculation with the analytical result.

## 9.2 An elliptical inclusion

As a second comparison we look at an elastic ellipse with principal axes  $R_x$  and  $R_y$  and elastic moduli  $\kappa_2 = 10$  and  $\mu_2 = 4$  embedded in an elastic plane with moduli  $\kappa_1 = 2.5$  and  $\mu_1 = 1$ . The crack starts at  $\gamma_s = R_x$ , follows the interface counter clock-wise and ends at  $\gamma_e = -R_x$ . Chen and Nakamichi have computed stress intensity factors for this setup at  $\gamma_e$  for aspect ratios  $R_y/R_x = 0.5$ ,  $R_y/R_x = 1$ , and  $R_y/R_x = 2$ . Data for  $F_{II}$  is presented graphically in the authors' Figure 7 as  $F_{II} = 0.69$ ,  $F_{II} = 0.69$ , and  $F_{II} = 0.51$  for the three aspect ratios, respectively. With ten panels on each crack and ten iterations in the GMRES solver we get  $F_{II} = 0.837747629930$ ,  $F_{II} = 0.6772186672348$ , and  $F_{II} = 0.5117664818436$ , both with the formulation of equation (51) and the formulation of equation (52). Since the data of Chen and Nakamichi and our computations typically only differ by a few per cent, we speculate that there is some mistake in the plotting of the curve for aspect ratio  $R_y/R_x = 0.5$  in their figure 7. The computation time on a SUN Ultra 1 workstation was about three seconds per configuration.

## 9.3 A complex inclusion

In a more challenging example we look at a nineteen-armed inclusion parameterized by

$$z(t) = (1 + 0.2 \cos(19t))e^{it}, \quad 0 \leq t < 2\pi. \quad (58)$$

and depicted in Figure 1. The cracks starts at  $\gamma_s = z(0)$  and ends at  $\gamma_s = z(1.7)$  A uniaxial stress  $\sigma_{yy}^\infty$  is applied at infinity and the elastic moduli are  $\kappa_2 = 10$ ,  $\mu_2 = 4$ ,  $\kappa_1 = 2.5$  and  $\mu_1 = 1$  for the inclusion and for the elastic plane. As a measure of the complexity of the geometry we first compute the arclength of the crack and of the bond: with 80 panels evenly

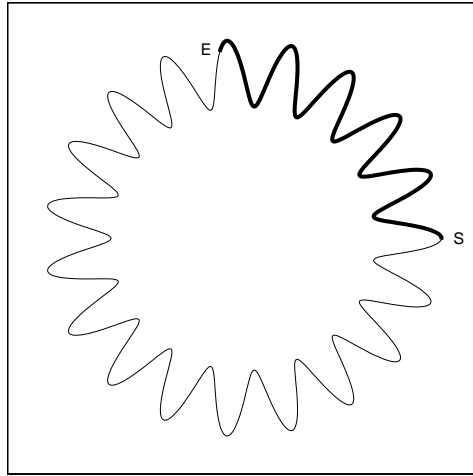


Figure 1: A crack along the interface of a nineteen-armed inclusion. The crack starts at 'S' and ends at 'E'.

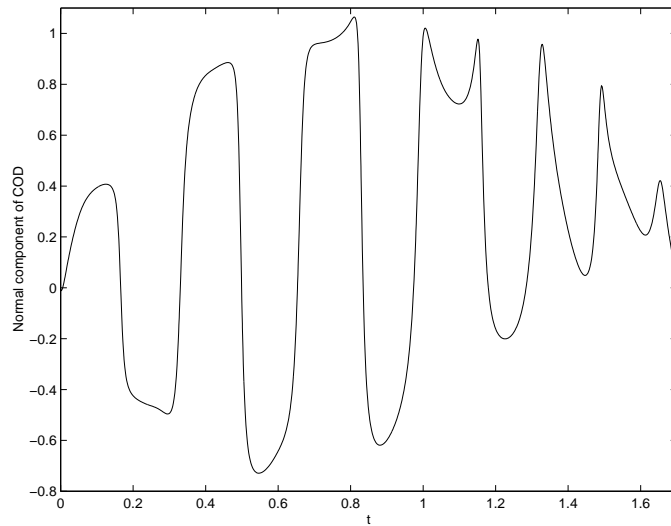


Figure 2: The normal component of the crack opening displacement versus interface parameter  $t$  of (58) for the crack in Figure 1 subjected to a uniform stress  $\sigma_{yy}^{\infty}$  at infinity.

distributed on the interface we get convergence of these quantities to 10 digits. With 160 panels we get 12 digits. Then we verify lemma (26) and (39) to 12 digits. This requires 100 panels. Finally, we compute stress intensity factors for crack-tip  $\gamma_s$ . With 80 panels and 55 iterations in the GMRES solver and the formulation (52) we get convergence to  $F_I = -0.0129561$  and  $F_{II} = -0.4053423$ . With 160 quadrature panels and 55 iterations we get convergence to  $F_I = -0.0129560788$  and  $F_{II} = -0.4053422716$ . The normal component of the crack opening displacement is plotted in Figure 2. Note that the opening has a negative sign on parts of the crack. The formulation of (51) gives a few digits less for the stress intensity factors. The computation time on a SUN Ultra 1 workstation for the largest computation is about fifteen minutes.

## 10 Discussion

This paper presents an efficient algorithm for the numerical solution to the elastostatic equation in a medium where there is an inclusion with an interface crack. The algorithm also computes stress intensity factors. The inclusion can have an arbitrary shape. The only user input that is needed is a parameterization of the inclusion interface. This is a major advantage over some previous methods which rely on geometry-specific fundamental solutions that could be very difficult to construct.

Our algorithm uses either of the two Fredholm equations (51), based on the upper-case potentials, and (52), based on the lower-case potentials. These equations perform rather similarly for the single interface crack, with a slight advantage for (52). The reason being that (52) has a smoother right hand side than (51) for curved interfaces. Another advantage with the lower-case potentials is that they give easy access to the crack opening displacement via (57).

Our algorithm is stable. High accuracy can be achieved, if desired. The asymptotic speed and storage requirements, however, are not completely satisfactory since, in the present implementation, the computing time and the need for storage grow quadratically with the number of discretization points needed to resolve the interface. Fortunately, there is a cure for this quadratic dependence: The fast multipole method or FMM [14, 15, 16] is a “matrix-free” approach to matrix-vector multiplication. Incorporating the FMM into the GMRES solver leads to a need for storage and a computing time that grows only linearly with the number of discretization points. Recently [8, 17] this was done for inclusions in the absence of cracks and for cracks in the absence of inclusions. Incorporating the FMM into our algorithm for an interface crack is a question of programming. We will attend to this in future work on cracks in more complex settings.

## Acknowledgements

This work was supported by NFR, TFR, and The Knut and Alice Wallenberg Foundation under TFR contract 96-977.

## References

- [1] A. H. England, 'An arc crack around a circular elastic inclusion' *J. Appl. Mech.* **88**, 637-640 (1966).
- [2] M. Toya, 'A crack along the interface of a circular inclusion embedded in an infinite solid', *J. Mech. Phys. Solids* **22**, 325-348 (1974).
- [3] M. Toya, 'Debonding along the interface of an elliptic rigid inclusion', *Int. J. Fracture* **11**, 989-1002 (1975).
- [4] D.-H. Chen and S. Nakamichi, 'Stress intensity factors for an interface crack along an elliptical inclusion' *Int. J. Fracture* **82** 131-152 (1996).
- [5] N. I. Muskhelishvili, *Some Basic Problems of the Mathematical Theory of Elasticity*, P. Noordhoff Ltd, Groningen (1953).
- [6] S. G. Mikhlin, *Integral equations*, Pergamon Press, London (1957).
- [7] L. M. Milne-Thompson, *Plane Elastic Systems*, Springer-Verlag, Berlin Heidelberg (1968).
- [8] L. Greengard and J. Helsing, 'On the Numerical Evaluation of Elastostatic Fields in Locally Isotropic Two-Dimensional Composites', *Courant Mathematics and Computing Laboratory* preprint 97-001 (1997).
- [9] J. Helsing and G. Peters, 'Integral equation methods and numerical solutions of crack and inclusion problems in planar elastostatics', *Department of Solid Mechanics KTH report 98-219* (1998).
- [10] N. I. Muskhelishvili, *Singular Integral Equations*, P. Noordhoff Ltd, Groningen (1953).
- [11] C. F. Shih, 'Cracks on bimaterial interfaces: elasticity and plasticity aspects', *Mater. Sci. Eng. A* **143** 77-90 (1991).
- [12] Y. Saad and M. H. Schultz, 'GMRES: a generalized minimum residual algorithm for solving nonsymmetric linear systems', *SIAM J. Sci. Stat. Comput.* **7**, 856-869 (1986).
- [13] A. B. Perlman and C. G. Sih, 'Elastostatic problems of curvilinear cracks bonded in dissimilar materials', *Int. J. Engn. Sci.* **5**, 845-865 (1967).
- [14] V. Rokhlin, 'Rapid solution of integral equations of classical potential theory', *J. Comput. Phys.* **60**, 187-207 (1985).
- [15] L. Greengard and V. Rokhlin, 'A fast algorithm for particle simulations', *J. Comput. Phys.* **73**, 325-348 (1987).
- [16] J. Carrier, L. Greengard, and V. Rokhlin, 'A fast adaptive multipole algorithm for particle simulations', *SIAM J. Sci. and Stat. Comput.* **9**, 669-686 (1988).
- [17] J. Helsing, 'Evaluation of stress fields in cracked planar elastic media', *Department of Solid Mechanics KTH report 97-211* (1997).